The oxidation of naphthalene and pyrene by cytochrome $P450_{cam}$

Paul A. England, Charles F. Harford-Cross, Julie-Anne Stevenson, Duncan A. Rouch, Luet-Lok Wong*

Department of Chemistry, Inorganic Chemistry Laboratory, South Parks Road, Oxford OX1 3QR, UK

Received 2 February 1998; revised version received 13 February 1998

Abstract Mutants of the heme monooxygenase cytochrome $P450_{cam}$ in which Y96 had been replaced with hydrophobic residues, have been shown to oxidise naphthalene and pyrene with rates one to two orders of magnitude faster than the wild-type. Naphthalene was oxidised to 1- and 2-naphthol, probably via the 1,2-oxide intermediate. In the case of the Y96F mutant, naphthalene was oxidised at a rate comparable to camphor. Pyrene oxidation gave 1,6- and 1,8-pyrenequinone with no evidence for attack at the *K*-region, in contrast to mammalian enzymes. The results show that the Y96 residue plays a key role in controlling the substrate range of $P450_{cam}$.

Key words: $P450_{cam}$; Monooxygenase; Mutagenesis; Protein engineering; Polycyclic aromatic hydrocarbon

1. Introduction

Polycyclic aromatic hydrocarbons (PAHs) are hazardous and recalcitrant environmental contaminants [1–3] mainly derived from the anthropogenic pyrolysis of organic matter such as fossil fuel consumption and coal-refining processes [4]. They are procarcinogens, being converted to highly carcinogenic oxidation products by the heme-dependent cytochrome P450 enzymes such as CYP1A1 [5]. P450 monooxygenases are also utilized for the initial oxidation step in the biodegradation of PAHs [6]. The PAH oxidation activity of P450 enzymes is therefore of wide interest, and we report here the oxidation of PAHs by genetically engineered forms of the heme monooxygenase cytochrome $P450_{cam}$.

Cytochrome $P450_{cam}$ (CYP101), which is found in the soil bacterium *Pseudomonas putida*, is the most well-characterised P450 monooxygenase [7–9]. We have investigated the protein engineering of $P450_{cam}$ for the oxidation of unnatural substrates [10–12]. In particular, we have shown that $P450_{cam}$ can be engineered by a single active site mutation, Y96A, to oxidise diphenylmethane which was not attacked by wild-type $P450_{cam}$ but was regio-specifically hydroxylated by the Y96A mutant to *para*-hydroxydiphenylmethane [13]. This was attributed to both the increased hydrophobicity of the substrate pocket and the possibility that the Y96A mutation generated space to accommodate diphenylmethane which is significantly larger than camphor. Since both these factors might also enhance the binding of PAHs, we investigated the oxidation of naphthalene and pyrene by mutants of $P450_{cam}$ in which Y96 had been replaced by the residues Gly, Ala, Val, and Phe, which have hydrophobic side chains of different sizes.

*Corresponding author. Fax: (44) (1865) 272690.
E-mail: LUET.WONG@CHEM.OX.AC.UK

2. Materials and methods

2.1. General

Buffer components were from Biometra. HPLC grade acetonitrile and chloroform, naphthalene, 1-naphthol, 2-naphthol, pyrene, and 1-hydroxypyrene were from Aldrich. UV/Vis spectra were recorded on a CARY 1E double-beam spectrophotometer. ^{1}H NMR spectra were recorded at 500 MHz on a Bruker WH500 or a Varian UnityPlus spectrometer. Gas chromatographic (GC) analyses were carried out on a Fisons Instruments 8000 series instrument equipped with a flame ionisation detector, using a DB-1 fused silica column (30 m × 0.25 mm i.d.). HPLC experiments were performed on a Gilson Gradient system using analytical (5 mm i.d. × 250 mm) or semi-prep (10 mm i.d. × 250 mm) C18 reverse phase columns and monitoring the eluents at 254 nm.

2.2. DNA manipulation and recombinant protein preparation

General DNA manipulation including site-directed mutagenesis [14], were carried out employing standard methods [15]. All possible mutations at the 96 position were generated using a degenerate oligonucleotide, and individual mutants were identified by DNA sequencing. Expression and purification of $P450_{cam}$ [16] and the associated electron transfer proteins putidaredoxin and putidaredoxin reductase [17,18] were carried out following literature methods. For wild-type $P450_{cam}$, only samples with purity ratio $A_{392}/A_{280} = 1.60$ were used [8]. The $P450_{cam}$ mutants did not show complete conversion of the heme to the high-spin state even in the presence of a large excess (1 mM) of camphor, and their purities were assessed by the ratio of the absorbances at 404 nm – the isosbestic point for the low-spin (417 nm)/high-spin (392 nm) conversion – and 280 nm. The minimum A_{404}/A_{280} ratio acceptable was 1.20, which corresponds to $A_{393}/A_{280} = 1.60$ for the wild-type enzyme.

2.3. NADH turnover rate measurements

Incubation mixtures (1.5 ml) in a cuvette contained 50 mM Tris-HCl buffer, pH 7.4, 1 μM $P450_{cam}$, 5 μM putidaredoxin, 1 μM putidaredoxin reductase and 200 mM KCl. Substrates were added as stocks in ethanol to a nominal final concentration of 100 μM. After equilibrating at 30°C for 2 min NADH was added to 200 μM and the absorbance at 340 nm was monitored. The NADH turnover rates were calculated using $\varepsilon_{340\ nm} = 6.22$ mM/cm.

2.4. Naphthalene oxidation

The 1-naphthol and 2-naphthol products were clearly resolved on the DB-1 GC column held at 120°C (retention times 1-naphthol: 24.4 min; 2-naphthol: 25.2 min). The GC detector response of the two naphthols at all column temperatures was identical, within experimental error.

Quantitative GC analysis was carried out at 200°C, because 1-naphthol and 2-naphthol have the same retention time on the DB-1 GC column at this temperature, which removed any uncertainties in integrating the small 2-naphthol peak. A standard solution of 1-naphthol was added to solutions (1.5 ml) containing all the components for an NADH turnover rate incubation except NADH and naphthalene, to give different final 1-naphthol concentrations. Each mixture was then extracted with 750 μl of chloroform at 4°C by thorough vortexing followed by centrifugation at 4000 × *g*, 4°C, for 20 min. An internal standard of *para*-hydroxydiphenylmethane was added to the extracts to a final concentration of 50 μM, and 1 μl of each sample was then analysed by GC at 200°C. A calibration curve of the peak area ratio of 1-naphthol to the internal standard vs. 1-naphthol concentration passed through the origin and was linear for the entire concentration range. The naphthalene turnover mixtures were then extracted and

PII S0014-5793(98)00189-6

analysed in an identical manner and the total naphthol product concentrations determined from the calibration curve.

2.5. Pyrene oxidation

The pyrene oxidation incubations were carried out on a 4-ml scale to increase the product concentrations for HPLC analysis. The reaction mixtures were extracted with 4 ml of $CHCl_3$ and, after centrifugation at $4000 \times g$, 4°C, for 20 min to separate the layers, 3 ml of the organic layer was removed. The $CHCl_3$ extract was evaporated under a stream of nitrogen and the residue redissolved in 1 ml of 40% (v/v) acetonitrile in water. A 400-μl aliquot was injected onto an analytical scale C18 reverse phase HPLC column, and a gradient of 40–50% (v/v) acetonitrile in water was developed over 30 min at a flow rate of 1 ml/min. The retention times of the major products were 13.5 min for 1,6-pyrenequinone and 14.3 min for 1,8-pyrenequinone.

To determine the relative activities of the $P450_{cam}$ enzymes towards pyrene oxidation, it was assumed that the extinction coefficients at 254 nm of the two pyrenequinones were identical. The ratio of the total product peak areas for different enzymes, standardized to an identical amount of NADH consumed in the reactions, gave the relative coupling efficiency of the $P450_{cam}$ enzymes. The relative PAH oxidation activities were then calculated by scaling to the reaction times.

For preparative scale incubations undertaken for product identification, the reaction volumes were increased to 50 ml and the incubations were carried out with stirring in 250-ml round bottomed flasks. The substrate and products were separated on a semi-prep C18 reverse phase HPLC column. The mobile phase was an acetonitrile/water mixture with a gradient of 40–50% acetonitrile being developed over 30 min at a flow rate of 3 ml/min.

3. Results

3.1. NADH turnover activities of the $P450_{cam}$ enzymes

The NADH consumption activities of the reconstituted $P450_{cam}$ system with camphor, naphthalene and pyrene as substrates are given in Tables 1 and 2. Wild-type $P450_{cam}$ had the lowest activity with both naphthalene and pyrene, and for all the $P450_{cam}$ enzymes studied the activity decreased with increasing size of the PAH. The NADH turnover rates of the Y96A and Y96F mutants with naphthalene as substrate were particularly high, and for the Y96F mutant it was faster than with camphor. However, since the monooxygenase activity of P450 enzymes is well known to undergo uncoupling side reactions [19,20], not all of the NADH consumed by the system was necessarily utilised for substrate oxidation [21]. It was therefore important to analyse the NADH turnover reactions for the presence of substrate oxidation products, and determine the quantities of products formed so that both the rate of product formation and consequently the coupling efficiency could be calculated.

3.2. The oxidation of naphthalene

Wild-type $P450_{cam}$ and all the Y96 mutants catalysed the oxidation of naphthalene to give a mixture of 1-naphthol and 2-naphthol, as confirmed by co-elution with authentic samples by GC. There was no evidence of further oxidation of the naphthols to catechols or other compounds. Analysis of authentic samples with identical concentrations of 1- and 2-naphthol showed that the two compounds gave the same GC detector response. Peak area integrations showed that all the $P450_{cam}$ enzymes investigated gave the same product ratio of $97 \pm 0.4\%$ 1-naphthol to $3 \pm 0.3\%$ 2-naphthol.

The concentration response of the GC flame-ionisation detector was calibrated with 1-naphthol to determine the amount of product formed and hence the rates of naphthalene oxidation by the $P450_{cam}$ enzymes. From these rates, the important parameter of coupling efficiency, i.e. the proportion of NADH molecules consumed which lead to substrate conversion, can be calculated. The naphthalene oxidation rates and the derived coupling efficiencies are listed in Table 1. All the Y96 mutants showed higher naphthalene oxidation rates than wild-type $P450_{cam}$. The Y96F mutant was the most active, with a naphthalene oxidation rate of 99.7 nmol Y96F/min and coupling efficiency of 55%. Although all the Y96 mutants showed much higher coupling efficiencies than wild-type $P450_{cam}$, there was no direct correlation with the NADH turnover rates. For instance the Y96A mutant showed much faster NADH turnover than the Y96G, but the two mutants have the same coupling efficiency of 17%. The coupling efficiency of 3% for wild-type $P450_{cam}$ was particularly low, and thus the combined effects of the much higher NADH turnover rates and coupling efficiencies increased the naphthalene oxidation rates of the Y96A and Y96F mutants to 30 and 142 times, respectively, of that of the wild-type enzyme. Indeed naphthalene was a comparable substrate to camphor in the case of the Y96F mutant.

3.3. The oxidation of pyrene

Pyrene oxidation by the $P450_{cam}$ enzymes gave one minor ($< 5\%$ by HPLC) and two major products; the two major products were purified by HPLC from a preparative scale incubation with the Y96A mutant. The ^1H NMR spectrum of both products showed resonances in the low-field region only. Comparison with literature ^1H NMR data showed that the two products were 1,6-pyrenequinone and 1,8-pyrenequinone [22].

Since the pyrenequinone products were not readily available, the *relative* rates of formation of the pyrenequinones and relative coupling efficiencies for wild-type $P450_{cam}$ and the Y96A and Y96F mutants were determined by HPLC, and the results are shown in Table 2. As observed with naphthalene, the greatly increased pyrene oxidation activity of the Y96A and Y96F mutants compared to wild-type $P450_{cam}$ arose primarily from the much higher (60- and 81-fold, respectively) coupling efficiencies of the mutants. From an estimate of the total amount of products isolated from the preparative scale incubation with the Y96A mutant, the total rate

Table 1
The rates and couplings of naphthalene oxidation catalysed by wild-type $P450_{cam}$ and the Y96 mutants

Naphthalene oxidation	Y96G	Y96A	Y96V	Y96F	WT
NADH turnover rate	47.3 ± 3.3	119 ± 9.7	51.8 ± 4.2	181 ± 9.8	23.9 ± 4.4
Coupling efficiency (%)	16.9 ± 0.9	17.0 ± 1.4	10.0 ± 0.7	55.0 ± 3.4	2.9 ± 0.2
Naphthalene oxidation rate	8.0 ± 0.3	20.2 ± 1.3	5.2 ± 0.5	99.7 ± 8.5	0.7 ± 0.2
Camphor oxidation rate	73.2 ± 4.5	155 ± 6.3	72.5 ± 5.8	160 ± 10.7	303 ± 20.5

All rates given as nmol $P450_{cam}$/min and all data as mean ± S.D. from 5 independent experiments. The camphor oxidation rates of the enzymes are included for comparison.

Table 2
The product distribution, relative rates and couplings of the oxidation of pyrene by wild-type $P450_{cam}$ and the Y96 mutants

Pyrene Oxidation	Product distribution for $P450_{cam}$ protein			
Products	Y96A	Y96V	Y96F	WT
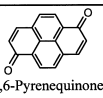 1,6-Pyrenequinone	48 ± 2%	35 ± 1%	60 ± 2%	52 ± 3%
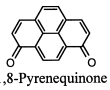 1,8-Pyrenequinone	52 ± 2%	65 ± 1%	40 ± 2%	48 ± 3%
NADH turnover rate	17.2±1.7	7.2±0.9	15.8±0.8	5.7±1.1
Relative coupling efficiency for quinone formation	60 ± 5	–	81 ± 10	1
Relative rate of quinone formation	180 ± 12	–	245 ± 18	1

All data given as mean ± S.D. from 6 independent experiments.

of formation of the pyrenequinones was calculated to be 0.5 nmol Y96A/min. The relative proportions of the two pyrenequinones formed by the different enzymes are given in Table 2. The data show that the $P450_{cam}$ enzymes had little selectivity between the two quinones.

The observation of 1,6- and 1,8-pyrenequinone from the oxidation of pyrene immediately suggested the involvement of the corresponding 1,6- and 1,8-dihydroxypyrenes as intermediates. These diols may in turn be formed by further oxidation of 1-hydroxypyrene arising from the initial attack on pyrene by the $P450_{cam}$ enzymes. The proposed 1,6- and 1,8-dihydroxypyrene intermediates are known to be susceptible to air oxidation to the quinones [22]. A 1-hydroxypyrene standard was well-resolved from the pyrenequinones on the HPLC column, but 1-hydroxypyrene was not detected even in the HPLC analysis of preparative scale incubations where the absorbance of the pyrenequinone peaks at 254 nm far exceeded 2 O.D. units. However, 1-hydroxypyrene was oxidized by all the $P450_{cam}$ enzymes, and 1,6- and 1,8-pyrenequinone were identified as the turnover products by HPLC. The fact that no 1-hydroxypyrene was observed could arise from either a very low steady-state concentration or very tight binding by the enzymes so that it did not dissociate from the enzyme active sites before being further oxidised.

4. Discussion

We have shown that $P450_{cam}$ can be re-engineered by mutation at a single active site residue to oxidise the polycyclic aromatic hydrocarbons naphthalene and pyrene. The present study, together with our earlier work [23], indicates that it is possible to engineer $P450_{cam}$ to oxidise unnatural substrates structurally unrelated to camphor, and that the Y96 residue plays a very important role in determining the substrate range of $P450_{cam}$.

The rates of naphthalene and pyrene oxidation by the Y96 mutants were one to two orders of magnitude faster than wild-type $P450_{cam}$. The striking observation was that naphthalene was a comparable substrate to camphor for the Y96F mutant (Table 1). The rate of oxidation of the more sterically demanding pyrene molecule was much slower (Table 2); the estimated activity of the Y96A mutant was only 0.5 nmol protein/min or 40-fold slower than the activity of this mutant towards naphthalene oxidation. Nevertheless, the pyrene oxidation activities of the $P450_{cam}$ mutants are comparable to the PAH oxidation activity of some rat [24] and human [25] P450 enzymes.

The data indicate that the coupling efficiency is an important factor in the enhancement of the rate of PAH oxidation by the Y96 mutants over wild-type $P450_{cam}$. This was especially evident for pyrene oxidation where the NADH turnover rates of the Y96A and Y96F mutants were only ca. 3 times that of the wild-type, but the 60-fold (Y96A) and 81-fold (Y96F) increases in coupling efficiency gave rise to the very large rate enhancements observed. The low coupling of 3% determined for the oxidation of naphthalene by wild-type $P450_{cam}$ is comparable to those observed for the oxidation of other unnatural substrates such as styrene and ethylbenzene (both ca. 5% [26,27]), and hexane (2% [11]). All the Y96 mutants showed substantially higher coupling for naphthalene oxidation than the wild-type, with the Y96F mutant being particularly effective (55%). These increased coupling efficiencies, together with the more modest increases in the NADH turnover rates, gave rise to the large overall enhancement of naphthalene oxidation activity.

The partition of uncoupling pathways in PAH oxidation catalysed by the $P450_{cam}$ enzymes between peroxide generation and oxidase activity was not determined. However, in most cases where the uncoupling has been determined, e.g. for the oxidation of styrene, ethylbenzene, and hexane by wild-type $P450_{cam}$, the dominant mechanism was the peroxide pathway [11,26,27]. Therefore, it is likely that the important factor here is the reduction of peroxide formation by the Y96 mutants. The increased hydrophobicity of the mutant active sites would disfavor water entry during the catalytic cycle, thus reducing uncoupling by the peroxide pathway [10]. However, active site hydrophobicity is not the only factor because the couplings varied between mutants but there was no obvious correlation with the side-chain volume at the 96 position.

The oxidation of PAHs by mammalian P450 enzymes has been investigated in detail because of the carcinogenicity of these compounds. Mammalian P450 enzymes oxidise PAHs to the arene oxides which rearrange by the NIH shift mechanism [28,29] to give isomeric phenols, although in some cases dihydrodiols are also formed [30]. In the presence of epoxide hydrolase, e.g. in oxidations by liver microsome or in vivo reactions, the epoxide is ring-opened to form the *trans*-dihydrodiols. In the presence of an inhibitor for epoxide hydrolase or for in vitro reactions, naphthalene oxidation gives predominantly 1-naphthol (> 90%) with varying amounts of 2-naphthol. We found that all the $P450_{cam}$ enzymes studied here oxidised naphthalene to give the same ratio of 1-naphthol (97%) to 2-naphthol (3%). This is completely consistent with the NIH shift rearrangement of a common naphthalene-1,2-oxide intermediate. Since the 1,2-oxide is the only initial product because the 2,3-oxide is too unstable, the results do not give any indication of the mode of naphthalene binding by mammalian P450s or the $P450_{cam}$ enzymes.

The oxidation of pyrene by mammalian P450 enzymes is complex and the products formed vary significantly between enzymes [31,32]. There are two sites of initial attack – the non-*K*-region 1,2-positions and the *K*-region 4,5-positions [24]. Further attacks on the initial products are also observed, in particular 1-hydroxypyrene is susceptible to further oxida-

tion at C6 and C8 [33]. In the oxidation of pyrene by different P450 enzymes induced in the rat liver by injections with various xenobiotics, the major product is either the *trans*-4,5-dihydrodiol or 1-hydroxypyrene, but the 1,6- and 1,8-diquinones can constitute up to 30% of the products [22,24,34]. Unlike their mammalian counterparts, the $P450_{cam}$ enzymes did not attack pyrene at the *K*-region 4,5-positions, nor was 1-hydroxypyrene observed in the products – the major products by far (>95% of total products) were the 1,6- and 1,8-pyrenequinones. This activity of the $P450_{cam}$ enzymes in fact resembles fungal metabolism of pyrene where attack at the *K*-region positions is not observed [35]. The major products observed in pyrene oxidation by the P450 enzyme from the fungus *Cunninghaemella elegans* arise from attack at the 1,6- and 1,8-positions, but in this case 1-hydroxypyrene is also observed as the minor product [22].

Since $P450_{cam}$ appears to follow the same mechanism of PAH oxidation as the mammalian enzymes, it can be assumed that the differences in selectivity of pyrene oxidation are due to the different modes of substrate binding. With the detailed knowledge of $P450_{cam}$ structure and mechanism built up over the last 30 yr, it can be envisaged that the $P450_{cam}$ active site could be engineered to achieve similar selectivities of PAH oxidation as the mammalian enzymes, especially the predominant attack at the *K*-region positions of pyrene. The ease of crystallization of $P450_{cam}$ may then allow the PAH binding orientation to be structurally characterized and compared with the proposed modes of PAH binding by mammalian enzymes such as CYP1A1 [31,32].

Acknowledgements: This work was supported by the Higher Education Funding Council for England (HEFCE), and a British Gas plc-Biotechnology Directorate–Clean Technology Unit–Department of Trade and Industry LINK programme. P.A.E., J.A.S. and C.F.H.C. thank the Engineering and Physical Sciences Research Council (UK) for Quota Studentships.

References

[1] Dipple, A. (1985) in: Polycyclic Hydrocarbons and Carcinogenesis (R.G. Harvey, Ed.) pp. 1–17, ACS Symposium Series 283, American Chemical Society, Washington, DC.
[2] Heitkamp, M.A. and Cerniglia, C.E. (1988) Appl. Environ. Microbiol. 54, 1612–1614.
[3] Schneider, J., Grosser, R., Jayasimhulu, K., Xur, W. and Warshawsky, D. (1996) Appl. Environ. Microbiol. 62, 13–19. and references herein
[4] Jacob, J., Karcher, W., Belliardo, J.J. and Wagstaffe, P.J. (1986) Fresenius Z. Anal. Chem. 323, 1–10.
[5] Guengerich, F.P. (1995) in: Cytochrome P450: Structure, Mechanism, and Biochemistry (Ortiz de Montellano, P.R., Ed.) pp. 473–536, Plenum Press, New York.
[6] Cerniglia, C.E. (1992) Biodegradation 3, 351–368.
[7] Mueller, E.J., Loida, P.J. and Sligar S.G. (1995) in: Cytochrome P450: Structure, Mechanism, and Biochemistry (Ortiz de Montellano, P.R., Ed.) pp. 83–124, Plenum Press, New York.
[8] Gunsalus, I.C. and Wagner, G.C. (1978) Methods Enzymol. 52, 166–188.
[9] Poulos, T.L., Finzel, B.C. and Howard, A.J. (1987) J. Mol. Biol. 195, 687–699.
[10] Nickerson, D.P., Harford-Cross, C.F., Fulcher, S.R. and Wong, L.-L. (1997) FEBS Lett. 405, 153–156.
[11] Stevenson, J.-A., Westlake, A.C.G., Whittock, C. and Wong, L.-L. (1996) J. Am. Chem. Soc. 118, 12846–12847.
[12] Bell, S.G., Rouch, D.A. and Wong, L.-L. (1997) J. Mol. Catal. B: Enzymatic 3, 293–302.
[13] Fowler, S.M., England, P.A., Westlake, A.C.G., Rouch, D.A., Nickerson, D.P., Blunt, C., Braybrook, D., West, S., Wong, L.-L. and Flitsch, S.L. (1994) J. Chem. Soc. Chem. Commun. 2761–2762.
[14] Kunkel, T.A. (1985) Proc. Natl. Acad. Sci. USA 82, 488–492.
[15] Sambrook, J., Fritsch, E.F. and Maniatas, T. (1989) Molecular Cloning: A Laboratory Manual, 2nd edn., Cold Spring Harbor Laboratory, Cold Spring Harbor, NY.
[16] Unger, B.P., Gunsalus, I.C. and Sligar, S.G. (1986) J. Biol. Chem. 261, 1158–1163.
[17] Peterson, J.A., Lorence, M.C. and Amarneh, B. (1990) J. Biol. Chem. 265, 6066–6073.
[18] Yasukochi, T., Okada, O., Hara, T., Sagara, Y., Sekimizu, K. and Horiuchi, T. (1994) Biochim. Biophys. Acta 1204, 84–90.
[19] Zhukov, A.A. and Arachov, A.I. (1982) Biochem. Biophys. Res. Commun. 109, 813–818.
[20] Kuthan, H. and Ullrich, V. (1982) Eur. J. Biochem. 126, 583–588.
[21] Gorsky, L.D., Koop, D.R. and Coon, M.J. (1984) J. Biol. Chem. 259, 6812–6817.
[22] Cerniglia, C.E., Kelly, D.W., Freeman, J.P. and Miller, D.W. (1986) Chem. Biol. Int. 57, 203–216.
[23] Wong, L.-L., Westlake, A.C.G. and Nickerson, D.P. (1997) Structure Bonding 88, 175–207.
[24] Jacob, J., Grimmer, G., Raab, G. and Schmoldt, A. (1982) Xenobiotica 12, 45–53.
[25] Shou, M., Grogan, J., Mancewicz, J.A., Krausz, K.W., Gonzalez, F.J., Gelboin, H.V. and Korzekwa, K.R. (1994) Biochemistry 33, 6450–6455.
[26] Fruetel, J.A., Collins, J.R., Camper, D.L., Loew, G.H. and Ortiz de Montellano, P.R. (1992) J. Am. Chem. Soc. 114, 6987–6993.
[27] Loida, P.J. and Sligar, S.G. (1993) Biochemistry 32, 11530–11538.
[28] Jerina, D.M. and Daly, J.W. (1974) Science 185, 573–582.
[29] Sono, M., Roach, M.P., Coulter, E.D. and Dawson, J.H. (1996) Chem. Rev. 96, 2841–2887.
[30] Jerina, D.M., Selander, H., Yagi, H., Wells, M.C., Davey, J.F., Mahadevan, V. and Gibson, D.T. (1976) J. Am. Chem. Soc. 98, 5988–5996.
[31] Miwa, G.T. and Lu, A.Y.H. (1986) in: Cytochrome P450: Structure, Mechanism, and Biochemistry (Ortiz de Montellano, P.R., Ed.) pp. 77–88, Plenum Press, New York.
[32] Jerina, D.M., Michaud, D.P., Feldman, R.J., Armstrong, R.N., Vyas, K.P., Thakker, D.R., Yagi, H., Thomas, P.E., Ryan, D.E. and Levin, W. (1982) in: Microsomes, Drug Oxidation, and Drug Toxicity (Sato, R. and Kato, R., Eds.) pp. 195–201, Japan Scientific Societies Press, Tokyo.
[33] Boyland, E. and Sims, P. (1964) Biochem. J. 90, 391–398.
[34] Okamoto, H. and Yoshida, D. (1981) Cancer Lett. 11, 215–220.
[35] Cerniglia, C.E. (1984) Adv. Appl. Microbiol. 30, 31–71.